RSC Advances

ROYAL SOCIETY OF CHEMISTRY

www.rsc.org/advances

Synthesis and physiochemical properties of novel gemini surfactants with phenyl-1,4-bis (carbamoylmethyl) spacer

Liyan Wang[a,b], Yue Zhang[a], Limin Ding[c], Jia Liu[a], Bing Zhao[a], Qigang Deng[a]* and Tie Yan[b]*

[a]*College of Chemistry and Chemical Engineering, Qiqihar University, Qiqihar, 161006, P. R. China*

[b]*Key Laboratory of Enhanced Oil & Gas Recovery, Ministry of Education, Northeast Petroleum University, Daqing,163318,P. R. China*

[c]*Cadre ward, Qiqihaer first Hospital, Qiqihar 161005, P. R. China*

* Correspondent. E-mail: wlydlm@126.com

A series of novel gemini surfactants, namely phenyl-1,4-bis [(carbamoylmethyl) N,N- dimethylalkyl ammonium chloride)] (a, b and c) were synthesized systematically and characterized by FT IR, ^{1}H NMR, ^{13}C NMR and MS. Their surface and bulk properties were evaluated by surface tension, conductivity, viscosity, dynamic light scattering (DLS) and transmission electron microscopy (TEM) measurements. These surfactants have been found to have low surface tension (γ_{CMC}) values as compared to other categories of gemini cationic surfactants and to form vesicles in solution at low concentration. The DLS and TEM studies showed that the aggregations of the above surfactants changed from larger globule vesicles and smaller globule micelles to network aggregates and then to globule vesicles with the increase of the surfactant concentration. It is assumed that this unusual aggregation behavior is related to the transformation of molecular conformation, phenyl-1,4-bis(carbamoylmethyl) spacer with rigidity and a hydrogen-bonding capability. The thermodynamic parameters of micellization process, namely, standard Gibbs free energy (ΔG^o_m), enthalpy (ΔH^o_m) and entropy (ΔS^o_m) were derived from conductivity measurement at different temperatures. Krafft points of three gemini surfactants are very low.

Gemini surfactants are amphiphilic molecules containing two hydrophilic head groups and two hydrophobic tails connected by a spacer at two head groups. Many studies have been carried out on gemini surfactants, focusing on their unique surface and bulk properties such as high surface activity, low critical micelle concentration(CMC), and more abundant self-assembly morphologies than the corresponding traditional single-chain surfactants.[1-4] Owing to these unique properties, gemini surfactants have been widely used in industrial detergency, the construction of high-porosity materials, templates for the synthesis of nanoparticles, nanorods, etc.[5-10] So, aggregation behavior of surfactants attract great attention in academic research.

The chemical structures of the gemini surfactants play an important role in their aggregation behavior.[11, 12] Especially, the nature of the spacer group (length, flexibility, polarity) has been shown to be of the utmost importance in determining the solution properties of aqueous gemini surfactants.[13, 14] These effects lead to the synergism of two alkyl tails of a gemini molecule, the change in the charge density of its headgroup, the variation of its molecule geometry by which rich structures and morphologies of aggregates yield, etc. More detailed, the flexible spacer influences the above functions of the gemini mainly depending on its length.[6,15] Too long flexible spacer can bend toward the alkyl tails so as to meet the chemical environment around the molecule, by which the molecule self-assembly is influenced. The effect of the short rigid spacer is almost identical with that of the flexible spacer having a similar length.[16] However, the long rigid spacer yields quite different effects from the flexible spacer owing to the two alkyl tails are inhibited to be close, which leads to the column-like molecular shape and the identical probability for the cis/trans configuration of the two alkyl tails around the spacer.[17,18] These make the gemini surfactant with long rigid spacer change aggregates morphology with increasing the gemini surfactant concentration or adding a few additives.[19,20] The chemical modification for the spacer is also discussed, which is expected to promote molecular self-assembly, or give some new functions to the aggregates.[21-24]

The most widely studied gemini surfactants are cationic alkanediyl-α,ω-bis (alkyldimethyl - ammonium) dibromide, which are referred to as CMC_sC_m , where m and s stand for the carbon atom number in the tail alkyl chain and in the methylene spacer, respectively. Previous studies had shown that the variation of the spacer and the tail alkyl chain usually affects the aggregation behavior of CMC_sC_m,[2,25] and the CMC_sC_m series ($4 \le s \le 12$, $12 \le m \le 16$) tends to form higher-curvature aggregates in aqueous solutions, such as spherical or elongated micelles.[26,27] Therefore, to design and synthesize a series of new gemini surfactants with phenyl-1,4-bis (carbamoylmethyl) as spacer (phenyl possesses rigidity and N-H can easy to form hydrogen bond) tend to form larger aggregates (vesicles and network aggregations) than micelles in aqueous solutions. Their properties such as surface activity, self-aggregation behavior were investigated, which would contribute to extend the potential application, such as templates for the synthesis of nanoparticles, nanorods, the synthesis of mesoporous material and so on.

In this paper, Gemini surfactants phenyl-1,4-bis [(carbamoylmethyl) N,N- dimethylalkyl ammonium chloride)] (**a, b** and **c**) have been synthesized. Their surface activity, thermodynamic property and aggregation behavior were evaluated by surface tension, electrical conductivity, transmission electron microscopy (TEM) and dynamic light scattering (DLS) techniques.

Experimental

Materials and instruments

All reagents were of analytical grade and used directly without further purification. Melting point (m.p) was measured by using X-6 micro melting point apparatus, Beijing Tektronix Instrument Company; FT-IR was obtained through using Nicolet750 infrared spectrometer, American Nicolet Company; ^{1}H NMR and ^{13}C NMR were recorded by using Avance 400 superconducting NMR, Switzerland Bruker

Company, DMSO and $CDCl_3$ used as the solvents; mass spectral analyses were carried out on an Agilent 7500 ESI-Ion Trop Mass spectrometer, American Agilent Company; surface tension was tested on a K100 Tensionmeter, Germany Kruss Company; conductivity was measured on Leici DDS-11A conductivity analyzer, Shanghai Leici Instrument Company; krafft temperature (T_K) was determined by heating the surfactant solution until a clear solution was obtained. All solution concentrations of these surfactants were 1 wt.% (i.e. well above the CMC of the investigated surfactants) using visual observation method.[15] DLS measurements were performed on a Malvern autosizer, Malvern, UK Company; TEM was obtained with an H-7650, Sitachi Instruments Company; relative viscosities were measured in two Ubbelohde viscometers thermostatted, Shanghai Huake equipment Company.

Synthesis of 1,4-bis(chloroethylamido)benzene

1,4-bis(chloroethylamido)benzene was synthesized according to the literature.[28] 2-chloroacetyl chloride (2mL, 25.0 mmol) was dissolved in chloroform (15 mL), then added dropwise to a stirred solution of 1,4-phenylene diamine (1.103 g, 10.0 mmol) and pyridine (2.1 mL, 25.0 mmol) in chloroform (30 mL). The pale purple solid was precipitated immediately. After stirred for 4 h under nitrogen atmosphere at room temperature, the pale purple solid was filtered, washed by saturated sodium bicarbonate solution and water respectively, dried and yielded 2.436 g of 1,4-bis(chloroethylamido)benzene. The synthesis of the gemini surfactants (**a**, **b** and **c**) is illustrated in Scheme 1.

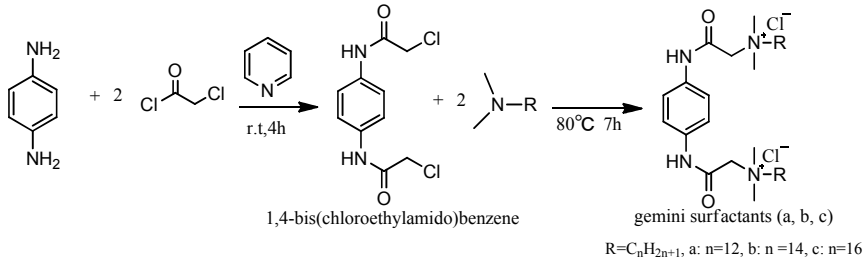

Scheme 1 Synthetic routes of gemini surfactants (**a**, **b** and **c**).

Characterization of 1,4-bis(chloroethylamido)benzene

1,4-bis(chloroethylamido)benzene yield. 92.98%. FT IR (KBr pellet) ν (cm^{-1}): 3 420 (N-H stretching, amino), 3 096 (C-H stretching, benzene ring), 2 952 (C-H stretching, methyl), 1 668 (C=O stretching, carbonyl), 1 595, 1 514, 1 407 (C=C stretching, benzene ring), 739 (C-Cl bending). ^{1}H NMR (600 MH_Z, DMSO), δ: 10.31 (s, 2H, N*H*), 7.53 (s, 4H, Ph*H*), 4.21 (s, 4H, O=C-CH_2-).

Synthesis of the gemini surfactants (a, b and c)

10.0 mmol of 1,4-bis(chloroethylamido)benzene and 30 mL of N,N-dimethylformamide (DMF) were added to a three-neck round-bottom flask, and 25.0 mmol of N,N-dimethyl alkylamine $(CH_3)_2NC_nH_{2n+1}$ (n = 12, 14, and 16) was added dropwise into the flask, then the mixture was stirred and reacted at 80℃ under nitrogen for 6-7 h. The resulting crude mixtures were cooled to 25℃. DMF was removed from the crude reaction mixture under reduced pressure in rotary flash evaporator at 80℃. It was then allowed to cool. The solid product was purified by recrystallization from mixtures of ethyl acetate and chloroform for five times to give each the gemini surfactants (**a**, **b** and **c**) as white solids and then dried in a vacuum oven for 5-6 h at 40℃. The yields were 68.82%, 71.64%, and 72.97% for **a**, **b** and **c**, respectively. The synthesis process was shown in Scheme 1. The structures of all products were confirmed by the characterization of FI-IR, ^{1}H NMR, ^{13}C NMR and ESI-MS.

Characterization of the gemini surfactants (a, b and c)

Phenyl-1,4-bis[(carbamoylmethyl)-N,N-dimethyldodecyl ammonium chloride)] a: White solid, m.p.: 204.2-205.4℃. FT IR (KBr pellet) ν (cm^{-1}): 3 497 (N-H stretching, amino), 3 027 (C-H stretching, benzene ring), 2 920 (C-H stretching, methyl), 2 851 (C-H stretching, methylene), 1 680 (C=O stretching, carbonyl), 1 563, 1 520, 1 470 (C=C stretching, benzene ring), 1 418 (C-H bending, methyl), 721 (alkyl chain bending, methylene). ^{1}H NMR (400 MH_Z, $CDCl_3$), δ: 11.09 (s, 2H, N*H*), 7.51 (s, 4H, Ph*H*), 4.87 (s, 4H, CH_2N^+), 3.69 (br s, 4H, $N^+CH_2CH_2$), 3.48 (s, 12H, N^+CH_3), 1.80 (m, 4H, $N^+CH_2CH_2$), 1.24-1.34 (m, 36H, alkyl chain), 0.87 (t, J = 6.8 Hz, 6H, CH_3). ^{13}C NMR (150 MH_Z, $CDCl_3$), δ (*10^{-6}): 161.12, 134.18, 120.58, 65.78, 63.87, 51.98, 31.90, 29.58, 29.43, 29.38, 29.32, 29.14, 26.26, 22.96, 22.68, 14.13. ESI MS (positive ions) m/z: found 615. 6 for $[M\text{-}2Cl\text{-}H]^+$, 308.3 for $[M\text{-}2Cl]^{2+}$.

Phenyl-1,4-bis[(carbamoylmethyl)-N,N-dimethyltetradecyl ammonium chloride)] b: White solid, m.p.: 210.1-212.2℃. FT IR (KBr pellet) ν (cm^{-1}): 3 456 (N-H stretching, amino), 3 080 (C-H stretching, benzene ring), 2 917 (C-H stretching, methyl), 2 850 (C-H stretching, methylene), 1 683 (C=O stretching, carbonyl), 1 588, 1 517, 1 470 (C=C stretching, benzene ring), 1 415 (C-H bending, methyl), 720 (alkyl chain bending, methylene). ^{1}H NMR (400 MH_Z, $CDCl_3$), δ: 11.11 (s, 2H, N*H*), 7.52 (s, 4H, Ph*H*), 4.88 (s, 4H, CH_2N^+), 3.69 (br s, 4H, $N^+CH_2CH_2$), 3.49 (s, 12H, N^+CH_3), 1.81 (m, 4H, $N^+CH_2CH_2$), 1.21-1.35 (m, 44H, alkyl chain), 0.87 (t, J = 6.8 Hz, 6H, CH_3). ^{13}C NMR (150 MH_Z, $CDCl_3$), δ (*10^{-6}): 161.13, 134.16, 120.59, 65.80, 63.88, 51.97, 31.93, 29.67, 29.65, 29.59, 29.44, 29.39, 29.36, 29.15, 26.26, 22.96, 22.69, 14.13. ESI MS (positive ions) m/z: found 671.6 for $[M\text{-}2Cl\text{-}H]^+$, 336.3 for $[M\text{-}2Cl]^{2+}$.

Phenyl-1,4-bis[(carbamoylmethyl)-N,N-dimethylhexadecyl ammonium chloride)] c: White solid, m.p.: 204.1-205.4℃. FT IR (KBr pellet) ν (cm^{-1}): 3 434 (N-H stretching, amino), 3 019 (C-H stretching, benzene ring), 2 955, 2 921 (C-H stretching, methyl), 2 851 (C-H stretching, methylene), 1 682 (C=O stretching, carbonyl), 1 574, 1 513, 1 469 (C=C stretching, benzene ring), 1 404 (C-H bending, methyl),

723 (alkyl chain bending, methylene). ^{1}H NMR (400 MH_Z, $CDCl_3$), δ: 11.25 (s, 2H, N*H*), 7.55 (s, 4H, Ph*H*), 4.89 (s, 4H, CH_2N^+), 3.68 (t, J = 8.0 Hz, 4H, $N^+CH_2CH_2$), 3.50 (s, 12H, N^+CH_3), 1.81 (m, 4H, $N^+CH_2CH_2$), 1.25-1.36 (m, 52H, alkyl chain), 0.88 (t, J = 6.8 Hz, 6H, CH_3).^{13}C NMR (150 MH_Z, $CDCl_3$), δ (*10^{-6}): 161.12, 134.15, 120.60, 65.80, 63.89, 51.98, 31.93, 29.71, 29.69, 29.67, 29.65, 29.60, 29.45, 29.40, 29.37, 29.16, 26.27, 22.97, 22.70, 14.13. ESI MS (positive ions) m/z: found 727.7 for $[M\text{-}2Cl\text{-}H]^+$, 364.4 for$[M\text{-}2Cl]^{2+}$.

Krafft point

The Krafft temperature (T_K) was determined by heating the surfactant solution until a clear solution was obtained. All solution concentrations of these surfactants were 1 wt.% (i.e. well above the CMC of the investigated surfactants) using visual observation method.[15]

Surface tension

The surface tension of the surfactant solutions were measured by the ring method using Krüss K100 Tensiometer (Krüss, Germany). The measurement temperature was controlled at 25.0±0.1℃ using a thermostatic bath. The tensiometer was calibrated using ultrapure water. The experiment was conducted from high concentrations to low concentrations.

Conductivity

The conductivity of the surfactant solutions was measured using a DDS-11A conductivity meter (Shanghai Leici Instrument Co.) with a Shanghai Leici DJS-1 conductivity electrode. Ultrapure water was added to the surfactant solution in order to change the surfactant concentration. The solutions were thermostated at 25.0±0.1, 35.0±0.1, 45.0±0.1 and 55.0±0.1℃ in a thermostatic bath.

Dynamic light scattering (DLS)

DLS measurements were performed on a Malvern autosizer (ZETASIZER nano series Nano ZS-90, Malvern, UK) at 90° scattering angle. All measurements were performed at 25.0±0.1℃.

Transmission electron microscopy (TEM)

Micrographs were obtained with an H-7650 (SITACHI Co.) transmission electron microscope at a working voltage of 100 kV. The TEM samples were prepared by the negative-staining method. Phosphotungstic acid solution (2%) was used as the staining agent. A carbon Formvarcoated copper grid (200 mesh) was placed on one drop of the sample solution for 5 min, and the excess solution was wiped away with filter paper to form a thin liquid film on the copper grid. Next, the copper grid was placed onto one drop of phosphotungstic acid solution for 2 min. The excess liquid was also wiped away with filter paper, and then the samples were dried in air.

Viscosity measurement

The relative viscosities of the surfactant solutions were measured in two Ubbelohde viscometers thermostatted at 25℃. The viscosities of all solutions were found to be independent of the capillary diameter and thus the flow rate.

Results and discussion

Krafft point

Krafft points of three gemini surfactants (**a**, **b** and **c**) were measured to insure the absolute dissolution in water at the experimental temperature. The krafft points of all of the Gemini surfactants (**a**, **b** and **c**) have been determined and found to be less 5℃ (Table 1), which are lower than that of the bis-N,N,N-dodecyldimethyl-p-phenylene diammonium dichloride,[29] it may result from the amide group being inserted into the spacer of gemini surfactants (**a**, **b** and **c**). Thus, the gemini surfactants have good solubility in water.

Table 1 Krafft points of three gemini surfactants (**a**, **b** and **c**)

gemini surfactants	**a**	**b**	**c**
Krafft point (℃)	<5	<5	<5

Surface activity

Surface activity of the gemini surfactants (**a**, **b** and **c**) was determined by surface tension measurements. The surface tension (γ) versus logC (i.e., C is the surfactant concentration) plot for the aqueous solutions of gemini surfactants (**a**, **b** and **c**) at 25℃ is shown in Fig. 1.

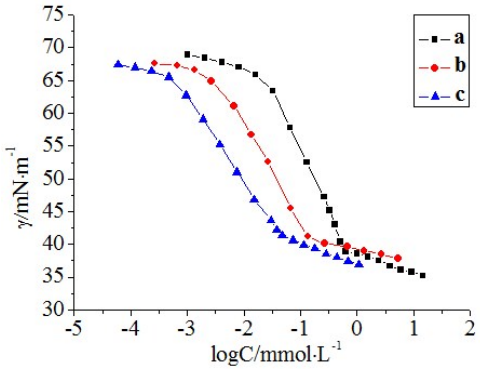

Fig.1 Curves of surface tension (γ) *vs*. log *C* of gemini surfactants (**a**, **b**, and **c**) at 25℃.

A plot of surface tension versus logC is often linear up to a concentration, called the critical micelle concentration (CMC), at which the surfactant begins to aggregate into a micelle. From Fig. 1, it can be found that with hydrophobic chain length increasing, the CMC value gradually decreased for the enhanced hydrophobic interaction between the longer alkyl chains (n = 12, 14 and 16). The surface parameters i.e., CMC, the surface tension attained at the CMC (γ_{CMC}), the effectiveness of surface tension reduction at CMC (π_{CMC}), the maximum surface excess concentration (Γ_{max}), the area per molecule at the interface (A_{min}), and the surfactant concentration required to reduce the surface tension of the solvent by 20 mN/m (C_{20}) of three gemini surfactants are given in Table 2. The packing densities of surfactants at the air-water interface are very important to interpret the surface activities of various surfactants.[14] The maximum surface excess concentration (Γ_{max}) [30] is defined as the maximum concentration of surfactant molecules at the interface of their solutions in the saturation case. It can be calculated by the following Eq. (1).

$$\Gamma_{max} = \frac{-1}{2.303nRT} \times \frac{d\gamma}{d\lg C} \quad (1)$$

Where, C is the concentration of surfactant aqueous solution, R is the gas constant (8.314 $J \cdot mol^{-1}K^{-1}$), T is the absolute temperature, and γ denotes the surface tension, n is the number of active species in the surfactant solution and equal to 3 (n = 3) in the case of gemini surfactants,[24] the results were listed in Table 2. It is clear from data that the gradual increase in the hydrophobic chain length decreases the concentration of the surfactant molecules at the interface.

The minimum area occupied per surfactant molecule (A_{min}) at the air-water interface is related to the maximum surface excess concentration (Γ_{max}) as following Eq. (2).

$$A_{min} = \frac{1}{N_A \times \Gamma_{max}} \quad (2)$$

Where, N_A is Avogadro's number.

Table 2 Surface activity parameters of the three new gemini surfactants and corresponding single chain surfactant (**a**, **b**, and **c**) at 25°C

Surfactants	CMC($molL^{-1}$)	γ_{CMC} ($mN\ m^{-1}$)	π_{CMC} ($mN\ m^{-1}$)	Γ_{max} ($\mu mol\ m^{-2}$)	A_{min} nm^2	C_{20} ($mol\ L^{-1}$)	CMC / C_{20}	pC_{20}
a	6.37×10^{-4}	38.97	33.03	0.93	1.78	1.43×10^{-4}	4.45	3.84
b	1.38×10^{-4}	40.70	31.30	0.82	2.03	2.94×10^{-5}	4.69	4.53
c	4.58×10^{-5}	41.31	30.69	0.65	2.56	6.46×10^{-6}	7.09	5.19
BAC-12[a]	9.10×10^{-3}	38.0		1.64	1.01			2.850
BAC-14[a]	1.90×10^{-3}	39.2		1.59	1.05			3.368
BAC-16[a]	4.00×10^{-4}	39.6		1.46	1.14			4.134

BAC-12: Dodecyl dimethyl benzyl ammonium chloride, BAC-14: Tetradecyl dimethyl benzyl ammonium chloride, BAC-16: Hexadecyl dimethyl benzyl ammonium chloride.

[a]The data of corresponding single chain surfactant (BAC) reported in Ref. [31].

Table 2 shows that these surfactants have been found to be having a significantly lower critical micelle concentration (CMC), higher efficacy in reducing surface tension compared to other conventional surfactants.[31] With the hydrocarbon chain length increasing, the gemini surfactant molecules pack more loosely, thus the γ_{CMC} of **c** compound is more than that of **a** or **b** compound. [32] It is also quite clear that surface tension values of these surfactants (n = 12, 14, 16) are lower than the corresponding gemini surfactants of large diethyl ammonium headgroups,[14] which indicates the gemini surfactants (**a**, **b** and **c**) with higher surface activity. The gemini surfactants (**a**, **b** and **c**) have two alkyl chains, dimethyl ammonium headgroups, and spacer containing a -(C_6H_4)- and two amide groups. The γ_{CMC} of Et series were slightly

bigger than those of Me series, loose arrangement of molecules at air/water interface induced by bigger headgroup should account for this phenomenon.[15] Close arrangement of gemini surfactants (**a**, **b** and **c**) molecules at air/water interface induced by smaller headgroup and rigid spacer should account for this phenomenon of lower surface tension. The CMC values of the gemini surfactant**s** (**a**, **b**, and **c**) are significantly lower than that of conventional surfactants. The lower CMC of these gemini surfactants is largely attributed to the two alkyl chains and the long rigid spacer. The long rigid spacer of phenyl-1,4-bis (carbamoylmethyl) yields quite different effects from the flexible spacer owing to the two alkyl tails are inhibited to be close, which leads to the column-like molecular shape (Fig. 7a) and the identical probability for the cis/trans of configuration of the two alkyl tails around the spacer (Fig. 8). The longer hydrophobic chain is more prone to bend at air/water interface. These reasons make the surfactant molecules reach easily saturated adsorption at the interface. Thus, it can be seen that the CMC values decrease and A_{min} increase of the gemini surfactants as the tail carbon number is increased from 12 to 16 (Table 2).

The gemini surfactants (**a**, **b** and **c**) with para-phenyl was employed as the rigid spacer unit and with dimethyl ammonium headgroups. Dimethyl ammonium headgroups are small. So, A_{min} means of the gemini surfactants (**a**, **b** and **c**) are smaller than cationic gemini surfactants with diethylammonium headgroups.[14] Moreover, the longer hydrophobic chain is more prone to bend at air/water interface, which lead to surfactant molecules have larger occupied area at air/water interface.[33] From Table 2 data, Γ_{max} decreased but A_{min} increased with the increase of the hydrocarbon chain length, which suggested the gemini surfactant molecules (**a**, **b** and **c**) with longer hydrocarbon chain has lower packing densities at the air-water interface.

π_{CMC} is an indication of the effectiveness of surface tension reduction, and it can be used to evaluate the effectiveness of surfactant to lower the surface tension of water[32] (Here, $\pi_{CMC} = \gamma_0 - \gamma_{CMC}$, where γ_0 and γ_{CMC} are the surface tensions of water and the surfactant solution at the CMC, respectively). So the larger the value of π_{CMC} is, the higher the effectiveness of surfactant is. pC_{20} is obtained by using the Eq. (3):

$$pC_{20} = -\log C_{20} \qquad (3)$$

The values of pC_{20} and π_{CMC} were listed in Table 2. The efficiency parameter indicates the adsorption behavior of surfactant molecules at the interface. The larger the value of pC_{20}, the greater the tendency of surfactants is adsorbed.[34] The variation of pC_{20} indicated that the pC_{20} increased with the increase of hydrocarbon chain length increasing. However, the π_{CMC} decreased with the increase of hydrocarbon chain increasing. The results show that the gemini surfactants (**a**, **b** and **c**) with longer hydrocarbon chain has lower ability to reduce surface tension. The value of CMC/C_{20} ratio is to determine structural factors in the adsorption and micellization process. The surfactant with larger CMC/C_{20} ratio has greater tendency to adsorb at the interface than to form micelles in solution. From Table 2, it can be seen that the surfactant with the increase of hydrophobic chain length was easier to adsorb at the air/water interface than self-assemble in solution. The result was in accordance with the conclusion from the value of pC_{20}.

The chemical structures of the gemini surfactants play an important role for their surface activity. Especially, the nature of the spacer has been shown to be of the utmost importance in determining the properties of the gemini surfactants aqueous. Gemini surfactant molecules adopt different conformations depending on the spacer (length, flexibility). Gemini surfactants (**a**, **b** and **c**) have the unsaturated and conjugated rigid spacer. The gemini surfactants might assume a linear conformation that would place only one of its hydrophobic tails into the air, the other tail would be forced to dip entirely into the water (Fig. 2, A). Alternatively, the horseshoe conformation would place both chains into the air (Fig. 2, B), but they would be separated from one another by a distance equal to the length of the spacer. Finally, a gemini might prefer to lie flat on the water surface (Fig. 2, C), an orientation that would occupy an extraordinarily large surface area per molecule. A_{min} values of the gemini surfactants (a, b and c) are very larger (from 1.78-2.56 nm^2), which corresponds closely to 2.36 nm^2.[35] We thereby speculate that surfactant molecules are planar at the interface. The surfactant with longer hydrocarbon chain has lower surface concentration at the interface and higher hydrophobic character. Hence, hydrophobic chain length also has a great influence on surface activity of the gemini surfactants (**a**, **b** and **c**). Those are in good agreement with previously obtained surface activity parameters.

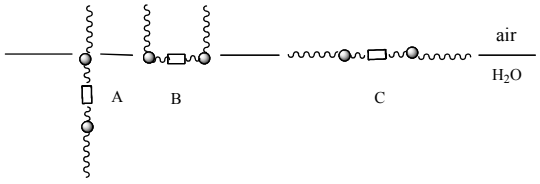

Fig.2. Possible orientations of the gemini surfactants (**a**, **b** and **c**) at an ais/water interface

Thermodynamics of Micellization

To obtain the micellization thermodynamics parameters of the gemini surfactants (**a**, **b** and **c**), the micellization behavior of the gemini surfactants (**a**, **b** and **c**) aqueous solutions at different temperature (25, 35, 45 and 55℃) was investigated by conductivity measurement. The electrical conductivity (κ) versus concentration (C) plots for the aqueous solutions of the gemini surfactants (**a**, **b** and **c**) are shown in Fig. 2.

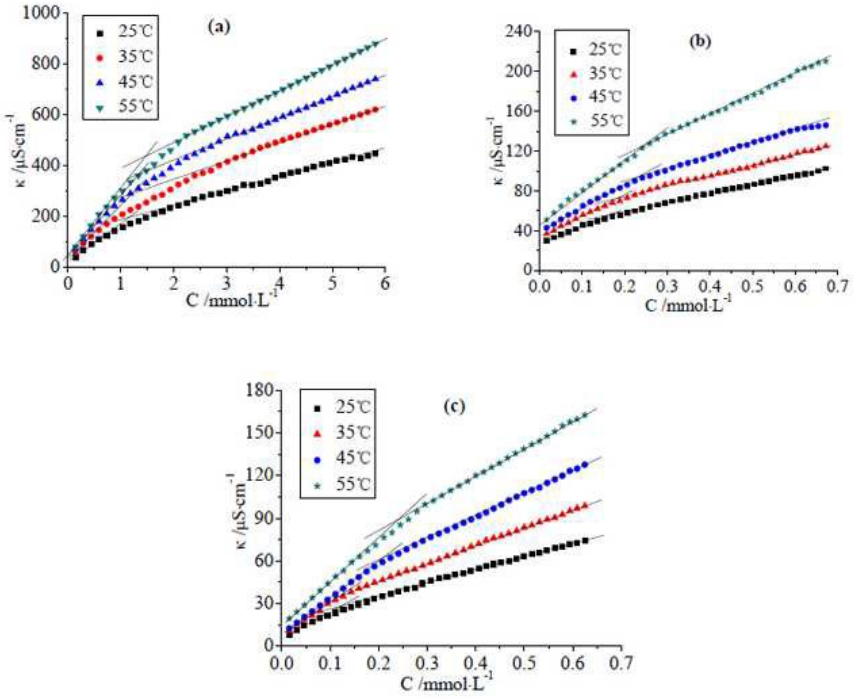

Fig. 3 Variation in the electrical conductivity (*κ*) with the gemini surfactants (**a**, **b** and **c**) concentration (C) at different temperature (25, 35, 45 and 55℃).

The CMC values were obtained from the intersection of two fitted liners in conductivity region. It has been observed that the CMC values of the gemini surfactants (**a**, **b** and **c**) increases with the increase of temperature (Fig. 3). The CMC values obtained by conductivity measurement are in good agreement with the surface tension derived data (Table 3). It is noteworthy that the CMC value of the gemini surfactants (**a**, **b** and **c**) obtained by this method is larger than that obtained by surface tension measurement (Table 2), which due to the existence of non-surface-active premicellar aggregates in gemini surfactants aqueous solutions. Similar results have been observed in other papers. [12]

Two opposite factors operated with temperature increasing [36]: (1) the ordered structure of water molecules around the hydrocarbon chain may be broken, which could promote solubilization of the surfactant monomer and thus disfavoring micellization; (2) the degree of hydrophilic hydration around the polar headgroup may decrease and thus favoring micellization. For the gemini surfactants (**a**, **b** and **c**), the former factor is predominant in micellization process in the studied temperature range.

Besides, the degree of counterion dissociation (α) was calculated from the ratio of the slops above and below CMC, respectively. The degree of counterion binding (β) could be obtained by Eq. (4). [33] β values were obtained from conductivity curves and listed in Table 3.

$$\beta = 1 - \alpha \tag{4}$$

The decrease of β with the increase of temperature meant the decrease of charge density on the micelle surface, which may be caused by a reduction in aggregation number of the gemini surfactants (**a**, **b** and **c**) micelles.

The thermodynamic parameters for micellization of the gemini surfactants (**a**, **b** and **c**) aqueous solutions can be calculated by the phase separation model. The standard Gibbs free energy (ΔG^{o}_{m}), enthalpy (ΔH^{o}_{m}), and entropy (ΔS^{o}_{m}) of micellization at different temperature were calculated by following Eq. (5)-(7).

$$\Delta G_m^0 = RT(0.5+\beta)\ln X_{cmc} \tag{5}$$

$$\Delta H_m^0 = -RT^2(0.5+\beta)\left(\frac{\mathrm{d}\ln X_{cmc}}{\mathrm{d}T}\right) \tag{6}$$

$$\Delta S_m^0 = \frac{\Delta H_m^0 - \Delta G_m^0}{T} \tag{7}$$

Where R is the gas constant (8.314 $J \cdot mol^{-1}K^{-1}$); T is absolute temperature; X_{CMC} is the CMC in molar fraction, X_{CMC}=CMC/55.4, where CMC is in mol/L, and 55.4 comes from 1 L of water corresponding to 55.4 mol of water at 298.15 K. Thus, T = 308.15 K, X_{CMC}=CMC/55.2; T = 318.15 K, X_{CMC}=CMC/55.0; T = 328.15 K, X_{CMC}=CMC/54.8. β is the degree of counterion binding to micelles. The values of $d\ln X_{CMC}/dT$ were obtained by fitting $\ln X_{CMC}$ - T a second-order polynomial.

The thermodynamic parameters i.e., ΔG^{o}_{m}, ΔH^{o}_{m} and ΔS^{o}_{m} of the gemini surfactants (**a**, **b** and **c**) at different temperature were listed in Table 3.

Table 3 The CMC and thermodynamic parameters of gemini surfactants (**a**, **b**, and **c**) determined by the electrical conductivity method at different temperatures.

Surfactants	T (K)	CMC (mmol L^{-1})	β	ΔG^0_m (kJ mol^{-1})	ΔH^0_m (kJ mol^{-1})	$T\Delta S^o_m$ (kJ mol^{-1})
a	298	1.17	0.69	-32.48	-7.38	25.11
	308	1.22	0.64	-31.37	-7.60	23.77
	318	1.35	0.63	-31.76	-8.02	23.74
	328	1.50	0.59	-31.13	-8.19	22.94
b	298	0.17	0.51	-31.67	-10.25	21.42
	308	0.18	0.48	-31.55	-10.64	20.91
	318	0.21	0.46	-31.57	-11.10	20.47
	328	0.25	0.43	-31.30	-11.53	19.77
c	298	0.10	0.50	-32.59	-11.16	21.43
	308	0.13	0.44	-31.20	-11.22	19.98
	318	0.20	0.39	-29.73	-11.36	18.37
	328	0.23	0.37	-29.67	-11.84	17.83

It can be seen that ΔG^o_m of micellization in all cases were negative and the negative values decreases with increase of temperature. The negative values of ΔG^o_m indicated that the micellization process was a thermodynamical spontaneous process. It can also be observed that ΔH^o_m were negative in all cases and decreased with the increase of temperature. The negative values of ΔH^o_m indicated that the micelle formation is exothermic process. As it is quite clear from Table 3 that the values for ΔH^o_m is smaller compared to $-T\Delta S^o_m$, thus the micellization process is entropy driven. This is true for all the gemini surfactants investigated in this studies.

Studies on the aggregation behavior

In order to study the aggregation behavior, the size distributions and morphologies of the aggregations formed for the gemini surfactant**s** at different concentrations were investigated by DLS and TEM, respectively. The chemical structures of the gemini surfactant **a** and **c** are analogous to **b**. So aggregation behavior of the gemini surfactant **b** is shown as example.

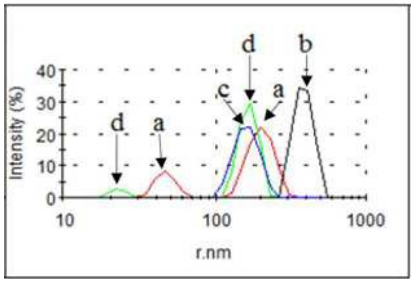

Fig. 4 DLS measurement of the size distributions of the gemini surfactant b at different concentrations: a. 5 times the CMC (red); b. 50 times the CMC (black); c. 100 times the CMC (blue); d. 50 times the CMC (0.1M NaCl) (green).

Fig. 4 shows the size distributions of the gemini surfactant **b** in solutions are described at 5 times the CMC, 50 times the CMC and 100 times the CMC by DLS. Fig. 4 shows that the size distributions range is about from 23 nm to 400 nm at different times of the CMC.

Fig. 4b (black curve) shows that there is one obvious peak with an average r of about 400 nm at 50 times the CMC for the surfactant **b**, reflecting the occurrence of large aggregations. However, there are two peaks with an average r of about 45 nm and of about 200 nm of the surfactant **b** at 5 times the CMC (Fig. 4a, red curve). Usually, the relative intensity of the larger size distributions is big and the relative intensity of the smaller size distributions is small. It reflects that lots of large aggregations and a small amount of micelles coexist at 5 times the CMC. Fig. 4c (blue curve) shows that there is one peak with an average r of about 170 nm at 100 times the CMC, which close to big peak of Fig. 4a. Thus, it may be existed large aggregations at 100 times the CMC.

The above results show that the relative intensity of the large size distribution began to increase then decreased with the increase of the surfactant concentration (from 5 CMC to 100 CMC).

In order to attain a direct visualization of above results, the morphologies of the gemini surfactant **b** at different concentrations were studied by TEM (Fig. 6).

It is well known that for a bilayer self-assembly, the hydrophobic chain modulates the phase behavior, whereas the head-group determines the bilayer surface chemistry. Intermolecular H-bonding between N-H and C=O in the amide group of spacer are responsible for the formation of spherical bilayer vesicles in dilute aqueous solution and has been reported earlier.[24] In fact, similar H-bonding interaction has been reported for many vesicles-forming surfactants.[37] The spacer of surfactants (**a**, **b** and **c**) containing amide group possesses the hydrogen-bonding capability. Hydrogen atom with oxygen atom of amide group form intermolecular hydrogen bonding of the surfactant molecules (Fig. 5). These H-bonding interactions near the headgroup region are able to minimize the repulsive interactions among the

cationic Me_2N^+ groups thus ensuring higher stability to the bilayer membrane. So, spherical vesicles with diverse sizes were observed for the surfactant **b** at 5 times the CMC (Fig. 6a, the left arrow mark small vesicle, the right arrow mark large vesicle), 50 times the CMC (Fig. 6c, the arrow mark), and 100 times the CMC (Fig. 6e, the arrow mark). Moreover visibly smaller globule micelles were also present at 5 times the CMC (Fig. 6b, the arrow mark). We thereby have reached the conclusion that the vesicles and micelles coexist at low concentration. The above results cohere with the DLS outcome.

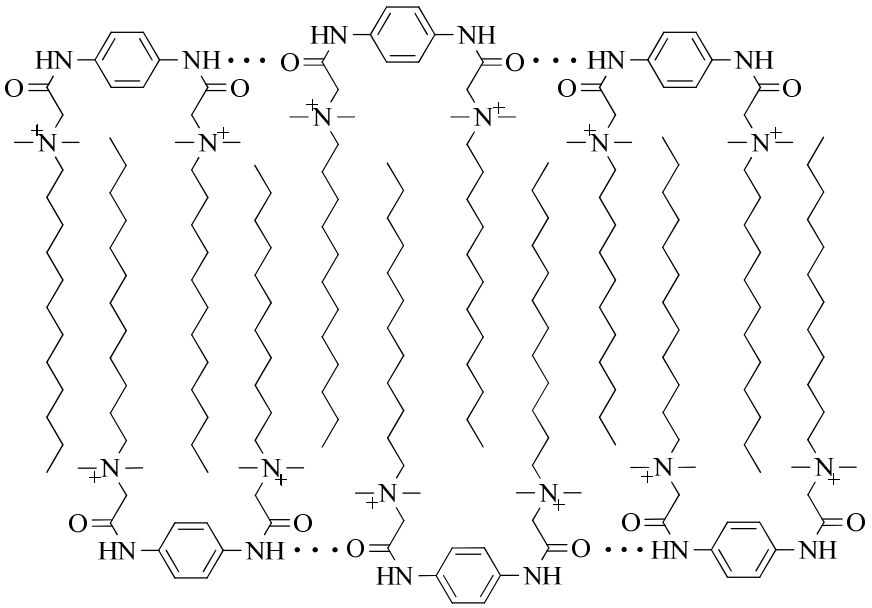

Fig. 5 Schematic representation of hydrogen bonding between different surfactant molecules.

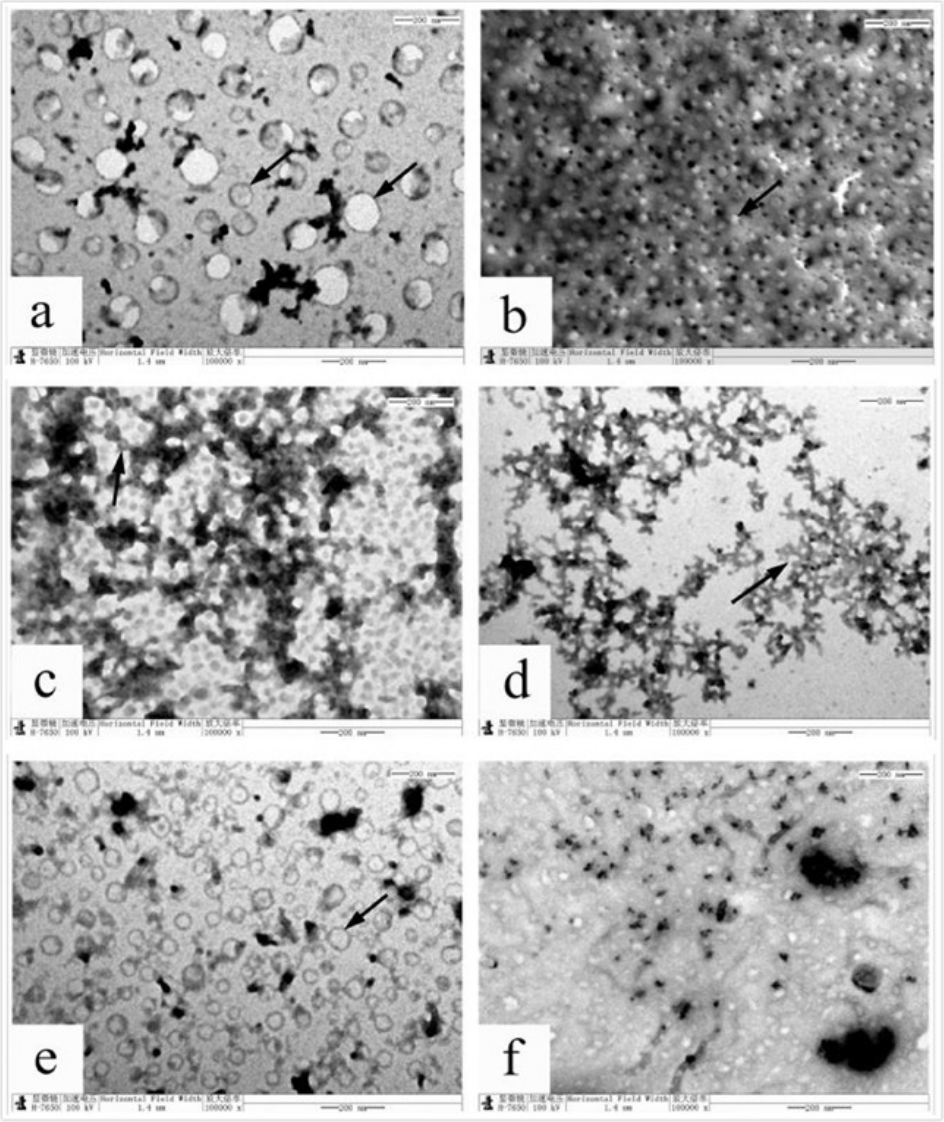

Fig. 6 TEM micrographs of a. 5 times the CMC, bar = 200 nm; b. 5 times the CMC, bar = 200 nm; c. 50 times the CMC, bar = 200 nm; d. 50 times the CMC, bar = 200 nm; e. 100 times the CMC, bar = 200 nm; f. 50 times the CMC (0.1M NaCl), bar = 200 nm.

The different spacers used will influence the molecule in a variety of ways. The distance between the charged nitrogen atoms will affect the charge density of the micelle and thus the degree of ionization. We thereby have thought that the formation of vesicles is also due to chemical structure of the spacer of the gemini surfactant. Phenyl-1,4-bis (carbamoylmethyl) as a long rigid spacer constrains the distance between the head groups, which inhibits the two alkyl tails to be close. Consequently, the surfactant molecules present mainly column-like molecular configuration (Fig. 7a), which can form vesicles. In addition, there is also a small amount of the surfactant molecules packing the hydrophobic tails tightly (Fig. 7b), which can form micelles at low concentration. [12]

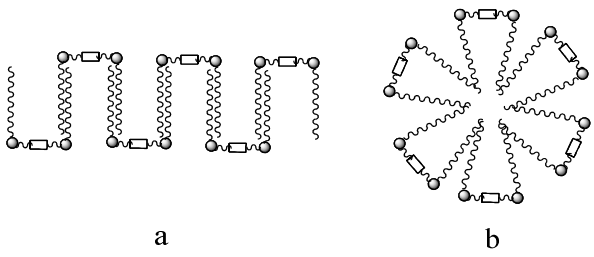

Fig. 7 Probable aggregation fashions of gemini surfactants with a long rigid spacer.

The DLS and TEM studies also show that the diverse sizes vesicles (Fig. 6a) and smaller micelles (Fig. 6b) transform into network aggregates (Fig. 6d) with increasing the gemini surfactant concentration (from 5 CMC to 50 CMC). Vesicles can be cross-linked together (Fig. 6c, the arrow mark) by trans configuration (Fig. 8b) and then formed the network aggregates at 50 times the CMC (Fig. 9). Usually,

surfactants first to form small aggregates at low concentrations, then the aggregates become larger with the increase of the surfactant concentration. In general, network aggregation should become larger at 100 times the CMC. However, this study results□are exactly opposite. There are lots of diverse sizes vesicles (Fig. 6e)□rather than larger aggregates at 100 times the CMC. This is an abnormal phenomenon. With the increase of the surfactant concentration (from 50 CMC to 100 CMC), trans configuration of alkyl tails (Fig. 8a) of surfactants molecular will transform into cis configuration of alkyl tails (Fig. 8a). The cis configuration of alkyl tails causes network aggregates disappear and transform into the vesicles.

We thereby have reached the conclusion, that diverse sizes vesicles may arise at low concentration and at high concentration.

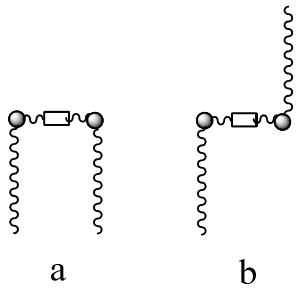

Fig.8 Cis(a) and trans(b) configurations of alkyl tails.

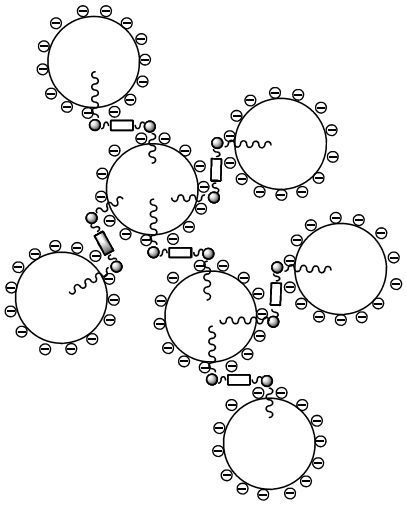

Fig. 9 Schematic representation of cross-linked vesicles by trans configurations of alkyl tails.

In order to further study the aggregation behavior, relative viscosity (relative to the water) of the gemini surfactant **b** was measured at different concentrations (Fig. 10**)**.

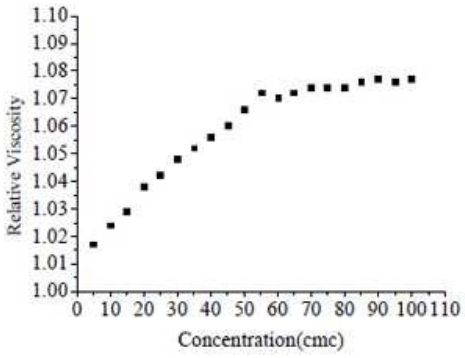

Fig. 10 Relative viscosity versus concentration of aniline surfactant b at 25□**.**

Fig.10 shows that the relative viscosity appeared rapid growth from 5 times the CMC to 50 times the CMC and very slow growth from 50 times the CMC to 100 times the CMC. At low concentration, adhesion and fusion of vesicles by trans configuration of alkyl tails lead to grow rapidly of viscosity. The results agree with the TEM outcome.

Effect of salt (NaCl) on network aggregates was investigated at the same time. In combination with the DLS results, it can be concluded

that network aggregates were destroyed and transformed into vesicles [size distributions (about 172 nm)] and micelles [size distributions (about 23 nm) (Fig. 4d, green curve)] in the aqueous solution of these gemini surfactants with 0.1 M NaCl addition. The TEM and DLS results all showed that the network aggregations indeed disappeared at 50 times the CMC with the 0.1M NaCl addition (Fig. 6f). The results show that the network aggregates have a poor salt tolerance. In addition, adding NaCl increases the concentration of counterion (Cl^-), which inhibits the ionization of vesicles. Thus vesicles are difficult to form network aggregates.

Conclusions

In this study, a new series of gemini surfactants with phenyl-1,4-bis (carbamoylmethyl) have been synthesized, characterized, and investigated for their surface, thermodynamic, and thermal properties. They have lower CMC value than corresponding mono-chain surfactants, and the CMC value decreased with hydrophobic chain length increasing. The gemini surfactants with rigid spacer and longer hydrocarbon chain has lower packing density but higher efficiency of adsorption. They have low krafft points shows that they have good solubility in water. An interesting phenomenon, the DLS and TEM studies reflect that the surfactant concentration, spacer and configurations strongly affect the aggregation behavior of these surfactants, that is, diverse sizes spherical vesicles and smaller globule micelles form at low concentration (5 CMC), vesicles and micelles gradually transfer to network aggregates (50 CMC) and then to diverse sizes vesicles (100 CMC) with an increase of the surfactant concentration. The salt-induced network aggregate-to-vesicles transitions were also found in these novel cationic gemini surfactants systems. It has also been observed from the thermodynamical studies that the micellization of gemini surfactants is entropy driven.

Acknowledgments

This work was supported by the Foundation of the Program for Heilongjiang Province of China (No. 12541864 & 12511591), the Science & Technology of Heilongjiang Province of China (No. B201116), the Overseas Scholars Foundation of Scientific and Technical Agency of Heilongjiang province of China (No.LC2011C17), the Overseas Scholars Foundation of Ministry of Human Resources and Social Security of the People's Republic of China (No. [2011] 508), and the National Science Fundation of China (No. 81403067) for financial support of this study.

References

1 F. M. Menger and J. S. Keiper, *Angew. Chem. Int. Ed.*, 2000, **39**, 1906.

2 R. Zana, *Adv. Colloid Interface Sci.*, 2002, **97**, 205.

3 S. S. Kim, W. Z. Zhang and T. J. Pinnavaia, *Science*, 1998, **282**, 1302.

4 E. Alami, H. Levy and R. Zana, *Langmuir*, 1993, **9**, 940.

5 Q. Liu, M. L. Guo, Z. Nie, J. B. Yuan, J. Tan and S. Z. Yao, *Langmuir*, 2008, **24**, 1595.

6 M. S. Bakshi, S. Sachar, G. Kaur, P. Bhandari, G. Kaur, M. C. Biesinger, F. Possmayer and N. O. Petersen, *Cryst. Growth Des.*, 2008, **8**, 1713.

7 M. S. Bakshi, *Langmuir*, 2009, **25**, 12697.

8 G. M. Andres, P. J. Jorge, C. A. Enrique and T. Gloria, *Angew. Chem., Int. Ed.*, 2009, **48**, 9484.

9 J. Aguado, J. M. Escola and M. C. Castro, *Microporous Mesoporous Matter.*, 2010, **128**, 48.

10 Q. R. Chen, L. Han, C. B. Gao and S. N. Che, *Microporous Mesoporous Matter.*, 2010, **128**, 203.

11 T. Lu, F. Han, G. G. Mao, G. F. Lin, J. B. Huang, X. Huang, Y. L. Wang and H. L. Fu, *Langmuir*, 2007, **23**, 2932.

12 X. G. Liu, X. J. Xing and Z. N. Gao, *Colloids Surf. Physicochem. Eng. Asp.*, 2014, **457**, 374.

13 R. Zana, *J. Colloid Interf. Sci.*, 2002, **248**, 203.

14 Q. Zhang, Z. N. Gao, F. Xu, S. X. Tai, X. G. Liu, S. B. Mo and F. Niu, *Langmuir*, 2012, **28**, 11979.

15 T. Lu, Y. R. Lan, C. J. Liu. J. B. Huang and Y. L. Wang, *J. Colloid Interf. Sci.*, 2012, **377**, 222.

16 T. Lu and J. B. Huang, *Chin. Sci. Bull.*, 2007, **52**, 2618.

17 X. Y. Wang, J. B. Wang, Y. L. Wang and H. K. Yan, *Langmuir*, 2004, **20**, 53.

18 J.X. Zhao, *Progess in Chemistry*, 2014, **26**, 1339.

19 T. Lu, F. Han, Z. C. Li and J. B. Huang, *Langmuir*, 2006, **22**, 2045.

20 M. N. Wang, Y. X. Wang, D. F. Yu, Y. C. Han and Y. L. Wang, *Colloid Polym. Sci.*, 2013, **291**, 1613.

21 C. C. Zhou, X. H. Cheng, O. D. Zhao, S. Liu, C. J. Liu, J. D. Wang and J. B. Huang, *Soft Matter*, 2014, **10**, 8023.

22 J. Lv, W. H. Qiao and C. Q. Xiong, *Langmuir*, 2014, **30**, 8258.

23 S. S. Song, Q. S. Zheng, A. X. Song and J. C. Hao, *Langmuir*, 2012, **28**, 219.

24 T. Patra, S. Ghosh and J. Dey, *J. Colloid Interf. Sci.*, 2014, **436**, 138.

25 R. Zana, M. Benrraou and R. Rueff, *Langmuir*, 1991, **7**, 1072.

26 D. Danino, Y. Talmon and R. Zana, *Langmuir*, 1995, **11**, 1448.

27 A. B. Groswasser, R. Zana and Y. Talmon, *J. Phys. Chem. B*, 2000, **104**, 4005.

28 H, G. Lee, J. H. Lee, S. P. Jang, H. M. Park, S. J. Kim, Y. Kim, C. Kim and R. G. Harrison, *Tetrahedron*, 2011, **67**, 8073.

29 L. Mivehi, R. Bordes and K. Holmberg, *Langmuir*, 2011, **27**, 7549.

30 A. Rodriguez, M. M. Graciani, M. Munoz, I. Robina and M. L. Moya, *Langmuir*, 2006, **22**, 9519.

31 Y. Y. Zhang, X. F. Guo, L. H. Jia, L. B. Gao and P. Wu, *Joumal of Qiqihar University*, 2014, **30**, 1.

32 C. C. Ren, F. Wang, Z. Q. Zhang, H. H. Nie, N. Li and M. Cui, *Colloids Surf. Physicochem. Eng. Asp.*, 2015, **467**, 1.

33 L. M. Zhou, X. H. Jiang, Y. T. Li, Z. Chen and X. Q. Hu, Langmuir, 2007, 23, 11404.

34 L. Perez, A. Pinazo, M. J. Rosen and M. R. Infante, *Langmuir*, 1998, **14**, 2307.

35 F. M. Menger, C. A. Littau, *J. Am. Chem. SOC.*, 1993,**115**, 10083.

36 J. Luczak, C. Jungnickel, M. Joskowska, J. Thoming and J. Hupka, *J. Colloid Interf. Sci.*, 2009, **336**, 111.

37 M. Popov, C. Linder, R. J. Deckelbaum, S. Grinberg, I. H. Hansen, E. Shaubi and T. Waner, E. *J. Liposome Res.*, 2010, **20**, 147.